Photonic jet etching: Justifying the shape of optical fiber tip

Andri Abdurrochman, Julien Zelgowski, Sylvain Lecler, Frédéric Mermet, Bernard Tumbelaka, and Joël Fontaine

Citation: AIP Conference Proceedings **1712**, 030001 (2016); doi: 10.1063/1.4941866
View online: https://doi.org/10.1063/1.4941866
View Table of Contents: http://aip.scitation.org/toc/apc/1712/1
Published by the American Institute of Physics

Photonic Jet Etching: Justifying the Shape of Optical Fiber Tip

Andri Abdurrochman[1, 2, a)], Julien Zelgowski[2], Sylvain Lecler[2], Frédéric Mermet[3], Bernard Tumbelaka[1] and Joël Fontaine[4]

[1]*Department of Physics, Faculty of Mathematics and Natural Sciences, Universitas Padjadjaran, Jl. Raya Bandung-Sumendang KM. 21 Jatinangor, Sumedang 45363, Indonesia.*
[2]*ICube-IPP, Université de Strasbourg, Pole API, 300 Boulevard Sébastien Brant, BP 10413, 67412 Illkirch, Strasbourg, France*
[3]Irépa Laser, *Pole API, Boulevard Sébastien Brant, 67412 Illkirch, Strasbourg, France*
[4]*ICube-IPP, INSA de Strasbourg, Boulevard de Victoire, 67000 Strasbourg, France.*

[a)]Corresponding author: a.andri@phys.unpad.ac.id

Abstract. Photonic jet (PJ) is a low diverging and highly concentrated beam in the shadow side of dielectric particle (cylinder or sphere). The concentration can be more than 200 times higher than the incidence wave. It is a non-resonance phenomenon in the near-field can propagate in a few wavelengths. Many potential applications have been proposed, including PJ etching. Hence, a guided-beam is considered increasing the PJ mobility control. While the others used a combination of classical optical fibers and spheres, we are concerned on a classical optical fiber with spherical tip to generate the PJ. This PJ driven waveguide has been realized using Gaussian mode beam inside the core. It has different variable parameters compared to classical PJ, which will be discussed in correlation with the etching demonstrations. The parameters dependency between the tip and PJ properties are complex; and theoretical aspect of this interaction will be exposed to justify the shape of our tip and optical fiber used in our demonstrations. Methods to achieve such a needed optical fiber tip will also be described. Finally the ability to generate PJ out of the shaped optical fiber will be experimentally demonstrated and the potential applications for material processing will be exposed.

INTRODUCTION: PHOTONIC JET ETCHING USING MICROSPHERES

Before it was coined as the photonic jet (PJ) in 2004, phenomenon in the near-field of spherical dielectric particle has already observed and proposed for surface processing using microspheres [1-6] for laser direct-etching. It has been demonstrated that microspheres on sample material can decrease the laser direct-etching, especially if the ultrafast (pico- or femto-seconds) lasers or shorter wavelength (ultra-violet range) lasers [7-13]. This decreasing size potency also has been demonstrated for nanosecond pulsed near-infrared lasers [14,15] that considered as more economical option than ultrafast pulsed ultra-violet lasers – not to mention its availability in well-packaged source. Using glass microspheres, this laser (28 ns of 1064 nm laser) which will not absorb much by a transparent glass is capable to etch glass slide. And on silicon wafer, this laser can decrease the LDE etching about 40 times smaller than LDE etching without glass microsphere; the smallest average diameter was around 1.3 µm using 4 µm glass microspheres with the laser fluence of 0.75 J/cm² and the PJ fluence of 43 J/cm².

The capability of PJ to obtain smaller LDE etching is understandable since PJ can focus (f_c) the beams into a very small beam size (Γ_{FWHM}) so it has folded intensities (I_{max}) propagate at a certain length (l_{FWHM}). These parameters are shown in Fig. 1.

Even though microspheres can be used for PJ etching, there are some drawbacks we must consider, e.g. microspheres are disposable; they can be used only once. And, there is no space or distance between microsphere and etched material, so material debris from the first ablation will contaminate the microsphere and avoids the following laser pulses to etch the material sequentially. Our observations revealed that two pulses is the least

2nd Padjadjaran International Physics Symposium 2015 (PIPS-2015)
AIP Conf. Proc. 1712, 030001-1–030001-6; doi: 10.1063/1.4941866

number of pulse needed to etch silicon wafer. We assume that the first pulse heats the surface and decreases the surface threshold fluence so the second pulse can etch the surface.

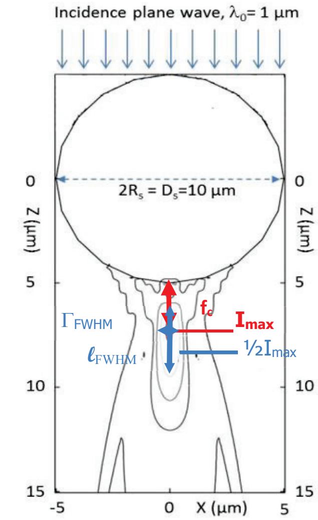

FIGURE 1. PJ is generated at the backside of glass microsphere with its parameters

But, the most important thing of using microsphere for PJ etching is: we cannot apply the highest PJ intensity I_{max} directly on the surface of material. We must make a distance between the surfaces (of sphere and material) around f_c if we wish to put I_{max} at the surface of material. In order to provide this space, a beam-trapping method has been proposed to trap the sphere using additional laser like in [10], but for practical used this method is too complicated. Therefore we propose an optical fiber with spherical-tip to be applied as the substitute of microspheres. And so the main objective of this manuscript is to justify the shape of optical fiber-tip for PJ etching.

WAVEGUIDE DRIVEN PJ

The possibility of generating PJ using such waveguide has already studied by simulating PJ from a planar waveguide for the case of radio-frequency wave [16]. For our case, we considered a planar optical fiber (n_{core} = 1.457 and n_{clad} = 1.44) and a Gaussian mode beam with the wavelength of 1 µm as the propagating wave inside the optical fiber. Also, the shape of optical fiber is considered to be circular, elliptical and pointed; with the core diameter of 10, 50 and 200 µm. The geometrical design of these optical fiber tips are depicted in Fig. 2.

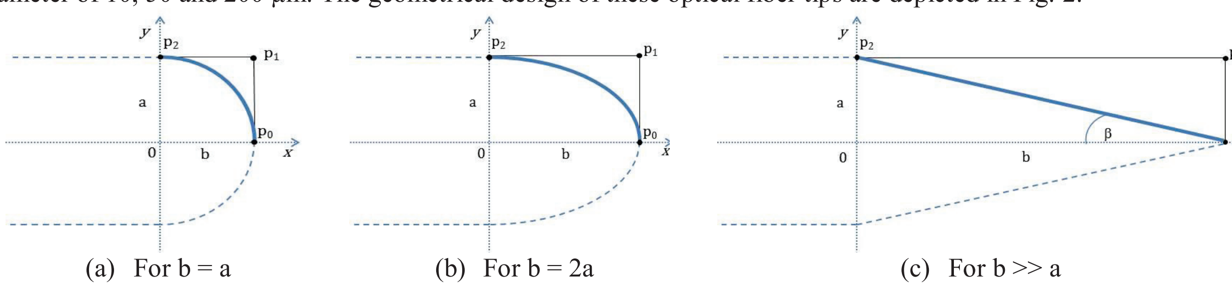

FIGURE 2. The shape of optical fiber tip considered to be (a) circular with axis ratio b=a, (b) elliptical with axis ration b=2a and (c) pointed with axis ratio b >> a

The mathematical function we used to define the shape is the rational quadratic Bézier curve function, with the general form [17]:

$$\mathrm{p}(t) = \frac{(1-t)^2 p_0 + 2(1-t)twp_1 + t^2 p_2}{(1-t)^2 + 2(1-t)tw + t^2}\ , \tag{1}$$

where w is the Bézier's weight curvature; $\boldsymbol{p}_0, \boldsymbol{p}_1$ and $\boldsymbol{p}_2$ are coordinates of three control points; and t is a parameter between 0 and 1. According to Fig. 2: $\boldsymbol{p}_0$= (b;0), $\boldsymbol{p}_1$= (b;a) and $\boldsymbol{p}_2$= (0;a). This function can create any curve depend to the Bézier's weight w, e.g. $w = 0.7$ for circular curve; therefore $w < 0.7$ corresponds to sharper tips, whereas $w = 1$ to rectangular one.

Our study here is conducted using finite element method, the same method as our colleague applied in their study [16], with respectively the tips are created with perfectly matched layer (PML) boundary condition around the free space and scattering boundary in the cladding. Figure 3 presents the simulation results for the case of core diameter 10 µm. Based on this figure and also other results for core diameter 50 and 200 µm, we drew some significance summaries:

1. Larger core diameters,
   a. Concentrate more electrical field; it is not only the fiber can collect more light, but also can propagate more modes;
   b. Concentrate the beam further from the tip surface;
   c. Generate larger beam spot (FWHM).
2. Elongated shape tip, e.g. elliptical, yields PJs closer to the tip with higher concentration than circular; when the axis ratio is getting larger, the beams will be concentrated inside the tip (Fig. 3.c) which can break the tip just like they broke $BaTiO_3$-spheres [14]. It makes the pointed shape is out of the option for practical use; the tip will be broken. Table 1 presents the PJs parameters generate by each waveguide size for circular and elliptical shape.
3. The elliptical shape generates PJ closer to the tip than circular one, so if this PJ is applied on the material some material debris can still pollute the tip; therefore for our study we consider only the circular shape.

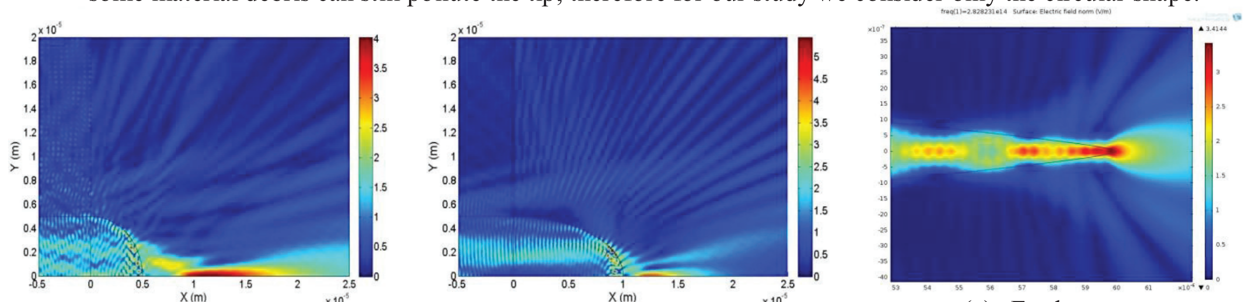

(a) For b = a (b) For b = 2a (c) For b >> a

FIGURE 3. PJs generated by 10 µm plane waveguide for the case of tip shape to be (a) circular with axis ratio b=a , (b) elliptical with axis ration b=2a and (c) pointed with axis ratio b >> a

TABLE 1. PJs parameters for each waveguide size and tip shape

Diameter of waveguide	Shape of the tip	Electrical field enhancement	Focal point from the tip (µm)	FWHM (µm)
10 µm	Circular	4.4	5.9	0.625
	Elliptical	6.5	2.3	0.625
50 µm	Circular	6.2	42.5	1.25
	Elliptical	8.1	20.5	1.25
200 µm	Circular	11.2	194	2.4
	Elliptical	22.5	94	1.2

FIRST PJ ETCHING USING OPTICAL FIBER

In practical use we must also consider the optical fiber for high power laser. We found that the smallest core of commercial optical fiber which can stand to high power laser has a diameter of 200 µm. This optical fiber is TEQS™ coated multimode fiber (Thorlabs®) with step refractive indexes (Fig. 4.a) and a numerical aperture of 0.22. The silica cladding is made from low-index fluorine-doped silica which provides superior near-infrared transmission. Whereas the TEQS™ secondary cladding provides a dual-waveguide designing, resulting in improved bend performance also allowing high-power handling capability. It can stand up to 0.2 kW for a continuous wave or 1.0 MW for a 10 ns Nd:YAG laser with a wavelength of 1064 nm and spot size of 80% of the core diameter. The tip of this TEQS™ coated multimode fiber then customized so it has as spheroid tip (Fig. 4.b).

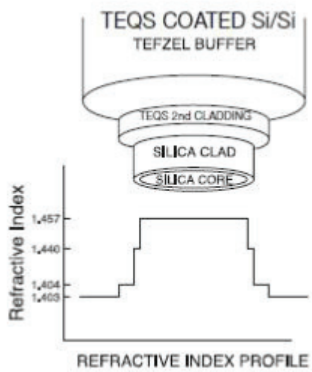

(a)

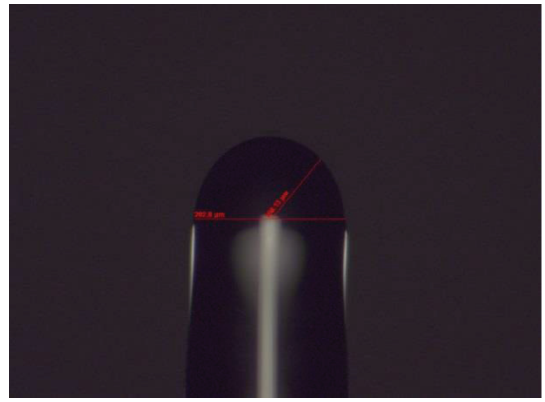

(b)

FIGURE 4. (a) Step refractive indexes of a TEQS^{TM} coated multimode fiber. (b) Spheroid tip of 200 µm TEQS^{TM} coated multimode fiber

This optical fiber is assembled in the experiment scheme (Fig. 5.a) with silicon wafer as the main sample material. A power meter was also added to measure the power of laser beam injected into the optical fiber at (a) and the power of PJ generated by the spheroid tip of optical fiber at (b). And, to provide a space between the optical fiber tip and sample material, we attached the optical fiber to a three-axis micro stage (Fig. 5.b). Next, (a) we move the tip directly on the sample surface; the indicate scale on the stage is considered as null space, then (b) we move the tip outward from the sample surface to any distance; the scale position is referred to the first scale and considered as the distance of material to the tip.

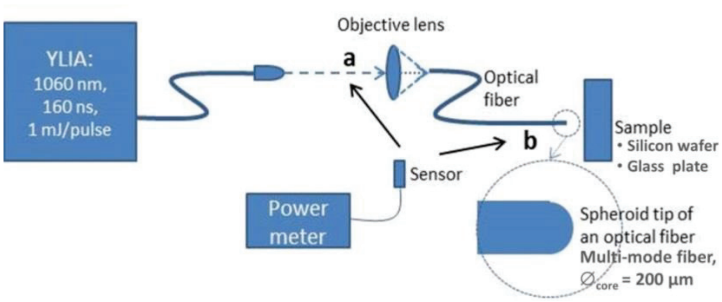

(a)

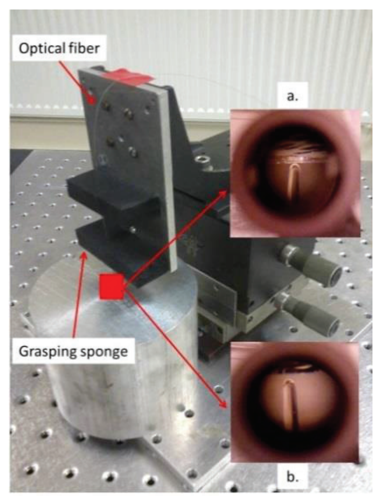

(b)

FIGURE 5. (a) Experiment scheme for PJ etching using spheroid tip fiber optics; the sensor at position (a) and (b) is for the laser beam and PJ measurement, respectively. (b) A three-axis micro stage is used to give a space between

In our study to demonstrate the PJ etching using optical fiber, we considered the laser system to be 160 ns of YLIA laser with the wavelength λ = 1060 nm, frequency rate f = 20 kHz and the maximum of average fluence $F_{\mathrm{max.av}}$ = 1 mJ/pulse. We also considered the distance between the tip and the sample at ≅ 75 µm. In addition to our main objective, i.e. first demonstration of PJ etching using optical fiber, we also collected the least number of pulses needed to achieve an etching mark on silicon wafer. These studies yielded the average sizes of PJ etching marks on silicon wafer as the function of the power of measured PJ and number of pulse (Table 2). We can see in the table that to achieve a PJ etching mark on silicon we need at least 4 pulses with the power of PJ 7.2 watts, which is generated by 19 watts of laser system (the maximum power of the YLIA laser). This etching mark has an average diameter of 17.5 µm can be seen in Fig. 6. This demonstration is sufficiently enough to provide the evidence of the potential application of PJ etching using optical fiber and justifying that the spheroid tip shape is working for the purpose.

TABLE 2. The average diameter of PJ etching marks on silicon wafer as a function of PJ power and number of pulse; created in the distance between the tip and silicon of 75 µm.

Injected power laser (watt)	Measured PJ power (watt)	PJ mark diameter (µm)					
		20 pulses	10 pulses	8 pulses	6 pulses	4 pulses	2 pulses
19	7.2	27.4	27.7	27.8	27.4	17.5	-
18.6	7.1	26.4	25.5	26.8	22.8	-	-
17.9	6.9	28.1	-	-	-	-	-
17.2	6.7	25.9	-	-	-	-	-
16.4	6.4	20.2	-	-	-	-	-

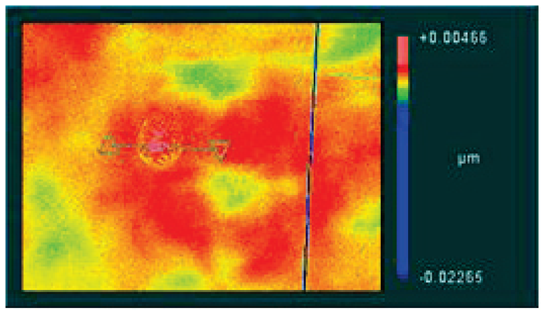

FIGURE 6. A PJ etching mark on silicon wafer captured by a profile-meter; created by 4 pulses of 7.2 watt PJ power at a distance of 75 µm

CONCLUSION

In this manuscript we report that the shape of optical fiber tip that for PJ etching should be spheroid. This shape has been justified using the simulation as well as experimental demonstrations, so the optical fiber can be used repeatedly. This spheroid shape keeps PJ's highest intensity outside the tip at a distance where the tip is safe from material debris in etching process. Even though, to obtain a good PJ etching using optical fiber, some parameters and variables must be optimized one to each other, e.g.: the parameters of the laser source, optical fiber and the curvature shape of the tip.

REFERENCES

1. Y. F. Lu, L. Zhang, W. D. Song, Y. W. Zheng and B. S. Luk'yanchuk, J. Exp. Theor. Phys. Lett. **72(9)**, 457-459 (2000).
2. M. Mosbacher, H. J. Munzer, J. Zimmermann, J. Solis, J. Boneberg and P. Leiderer, Appl. Phys. A- Mater. Sci. Proc. **72(1)**, 41-44 (2001).
3. H. J. Münzer, M. Mosbacher, M. Bertsch, J. Zimmermann, P. Leiderer and J. Boneberg, J. Microscopy **202(1)**, 129-135 (2001).
4. Y. Lu, S. Theppakuttai and S. C. Chen, Appl. Phys. Lett. **82(23)**, 4143-4145 (2003).
5. S. Theppakuttai and S. Chen, Appl. Phys. Lett. **83(4)**, 758-760 (2003).
6. S. M. Huang, M. H. Hong, B. S. Luk'yanchuk, Y. W. Zheng, W. D. Song, Y. F. Lu and T. C. Chong, J. Appl. Phys. **92(5)**, 2495-2500 (2002).
7. A. Chimmalgi, C. P. Grigoropoulos and K. Komvopoulos, J. Appl. Phys. **97(10)**, 104319(1)-104319(12) (2005).
8. W. Wu, A. Katsnelson, O. G. Memis and H. Mohseni, Nanotechnology **18(48)**, 485302-6 (2007).
9. W. Guo, Z. B. Wang, L. Li, D. J. Whitehead, B. S. Luk'yanchuk and Z. Liu, Appl. Phys. Lett. **90(24)**, 243101-3 (2007).
10. E. McLeod and C. B. Arnold, Nature Nanotechnology **3(7)**, 413-417 (2008).
11. A. Plech, P. Leiderer and J. Boneberg, Laser & Photonics Reviews **3(5)**, 435-451 (2009).

12. D. Grojo, L. Charmasson, A. Pereira, M. Sentis and P. Delaporte, J. Nanosci. Nanotechnol. **11(10)**, 9129-9135 (2011).
13. P. Delaporte, D. Grojo, L. Boarino, L. Charmasson, N. De Leo, K. L. N. Deepak, M. Laus, G. Panzarasa, A. Pereira, R. Rocci, K. Sparnacci and O. Uteza, presented at the 17th International School on Quantum Electronics - Laser Physics and Applications (ISQE), Nessebar, BULGARIA, 2012 (unpublished).
14. A. Abdurrochman, S. Lecler, J. Fontaine, F. Mermet, P. Meyrueis, B. Y. Tumbelaka and P. Montgomery, presented at the Photonic Europe 2014: Laser Sources and Applications II, Brussels, Belgium, 2014 (unpublished).
15. A. Abdurrochman, S. Lecler, F. Mermet, B. Y. Tumbelaka, B. Serio and J. Fontaine, Applied Optics **53(31)**, 7202-7207 (2014).
16. H. Halaq, S. Lecler, Y. Takakura, S. Robert and B. Sauviac, in *Workshop EM IEEE 2010* (IEEE, Saint-Malo, France, 2010).
17. G. Farin, Curves and Surfaces for CAGD: A Practical Guide, 5th ed. (Morgan Kaufmann, San Fransisco, 2002).